Charged cyclophanes with extended conjugation: the effect of the cyclophane hub on the charge distribution

E. Shabtai,[a] M. Rabinovitz,*[,a] B. König,[b] B. Knieriem[b] and A. de Meijere[b]

[a] *Department of Organic Chemistry, The Hebrew University of Jerusalem, Givat Ram, Jerusalem, Israel 91904*

[b] *Institut für Organische Chemie der Georg-August-Universität Göttingen, Tammannstrasse 2, D-37077 Göttingen, Germany*

Compounds 1, 2 and 3 were chemically reduced with lithium, sodium and potassium metals in [$^2H_8$]THF at 220 K. In each case the reversibility of the process was tested by quenching with molecular oxygen. The reduction of 1 with all three metals yields the corresponding tetraanion salt $1^{4-}/4M^+$. Compound 2 was reduced reversibly with potassium and sodium only, while compound 3 underwent decomposition. According to the UV–VIS spectra and the electrochemical results, the tetraanion species is formed *via* a stepwise four-electron transfer process. A strong effect of the cyclophane hub on the charge distribution *vis à vis* a relevant model system is demonstrated.

Introduction

One of the most intriguing questions related to cyclophanes is how the forced proximity of the two π systems influences their chemical and physical properties. In cyclophanes like [2.2]paracyclophane, the two benzene rings are held rigidly, face to face, at a short distance of *ca.* 3 Å.[1] This interdeck distance which is much smaller than the usual van der Waals interaction distance, between parallel aromatic hydrocarbons in the crystal,[2] is responsible for the unique behaviour of these systems.

Compound **1**, 4,7,12,15-tetrastyryl[2.2]paracyclophane, was

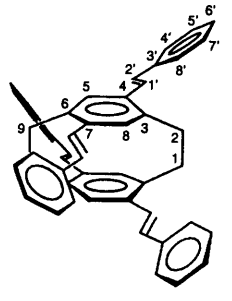

1

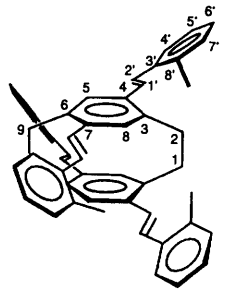

2

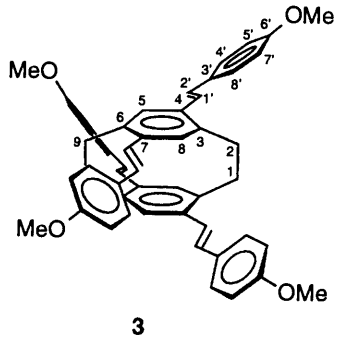

3

first synthesized and characterized by de Meijere *et al.*[3] As established by X-ray structure analysis, the molecular structure of **1** in the crystal exhibits a typical [2.2]paracyclophane centre. The interplanar angles between the phanearene and phenyl moieties in **1** vary from 42.3° to 55.8°, presumably as a result of the intermolecular order in the crystal. The styryl substituted groups which are arranged in a 'crossed' manner are tilted out of the phanearene plane, as a way of balancing steric hindrance and conjugation, within each deck.

According to NMR spectroscopy, it seems that the NMR parameters in **1** do not differ significantly from those of a 'normal' stilbene. There is free rotation of the terminal phenyl rings about the C-2′–C-3′ bond, even at 160 K. The coupling constant, $^3J_{HH}$ 16.3 Hz of the ethylene group protons is a typical value for a *trans* double bond, and the chemical shifts of the ethylene bridge and the phenyl rings are also typical.

The UV–VIS and fluorescence spectra of compound **1** reveal a red shift of the absorption and emission bands as compared with a reference system, *i.e.* 2,5-dimethyl-1,4-distyrylbenzene (**4**). This phenomenon, *i.e.* the fluorescence of excimers,[4] is

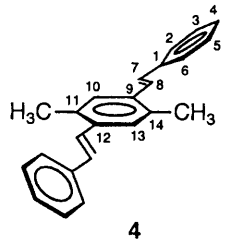

4

caused by strong electronic interactions between the two 1,4-distyryl chromophores across the central [2.2]paracyclophane. Transannular interactions between the benzene rings are particularly pronounced when the molecular bridges are short. Therefore, upon reduction, such a system is not expected to behave as being composed of two separate parts but rather as an integrated unit.

The degree of charging and the charge distribution pattern of charged systems can be studies by NMR. The relationship between ^{13}C chemical shifts and charge densities on the corresponding carbon atoms is expressed by eqn. (1),[5] where $\Delta\delta c_i$ is

$$\Delta\delta c_i = K_c \Delta q_i \quad (1)$$

the difference between the chemical shifts of a carbon atom c_i of the charged species and its neutral precursor, Δq_i is the charge on the carbon atom c_i in the charged species and K_c is a proportionality constant. Other effects, such as shielding and

Table 1 Displacement of carbon and proton chemical shifts (ppm) upon charging of **1** (top) and **2** (bottom)

Proton NMR bands displacement of **1**

M	6′	5′	7′	4′	8′	3′	2′	1′	4/7	5/8	3/6	2/9	2/9	Σδ∆
Li	2.20	1.15	1.35	1.41	1.73	—	2.81	1.64	—	1.73	—	1.04	0.45	62.3
Na	1.96	1.05	1.22	1.28	1.53	—	2.65	1.54	—	1.83	—	0.95	0.42	58.2
K	1.97	1.03	1.20	1.27	1.68	—	2.85	1.52	—	1.85	—	0.97	0.47	59.6

Carbon NMR bands displacement of **1**

M	6′	5′	7′	4′	8′	3′	2′	1′	4/7	5/8	3/6	2/9		Σδ∆
Li	24.6	0.4	1.8	15.5	7.3	−5.8	47.9	13.4	20.5	5.1	8.3	−0.6	—	553
Na	21.9	0.4	1.6	14.9	6.7	−6.1	49.4	14.3	23.8	8.1	7.0	−0.3	—	567
K	22.1	0.0	0.7	15.1	9.0	−4.8	47.4	13.6	22.5	6.0	7.5	−0.1	—	557

Proton NMR bands displacement of **2**

M	8′CH_3	8′	7′	6′	5′	4′	3′	2′	1′	4/7	5/8	3/6	2/9	2/9	Σδ∆
Na	0.38	—	0.82	1.63	0.79	1.16	—	3.02	1.09	—	1.68	—	0.78	0.3	49.6
K	0.32	—	0.78	1.60	0.76	1.18	—	3.16	1.11	—	1.75	—	0.74	0.33	49.5

Carbon NMR bands displacement of **2**

M	8′CH_3	8′	7′	6′	5′	4′	3′	2′	1′	4/7	5/8	3/6	2/9		Σδ∆
Na	−1.6	13.2	2.3	22.1	0.7	13.4	−5.1	49.6	15.0	23.6	8.6	6.8	−0.2	—	593
K	−1.4	14.4	1.7	21.3	0.4	13.6	−4.2	49.4	15.2	21.2	7.2	6.6	0.3	—	582

conformational changes, may be neglected because of the special crossed arrangement of the π systems and the typical rigid skeleton of such compounds.

Results and discussion

In order to study the influence of the cyclophane's hub on the properties of the charged species, we reduced compounds **1**, **2** and **3** with different metals and compared the change in their NMR chemical shifts with a suitably charged model. All three compounds were reduced *via* an electron transfer process with lithium, sodium and potassium metals in [$^2H_8$]THF at 220 K. In each case the validity of the charging process was tested by quenching with oxygen, to ensure that no skeletal changes had occurred. The reduction of **1** with all three metals yields the tetraanion salt $\mathbf{1}^{4-}/4M^+$. Compound **2** was reduced with potassium and sodium only, while compound **3** underwent decomposition. We assume that the methoxy groups are cleaved upon charging.[6] The carbon and hydrogen atoms were assigned by correlation spectroscopies, *e.g.* DQF-COSY, NOESY, CH-correlation, and long range CH-correlation. The changes in carbon and proton chemical shifts upon charging of **1** and **2** with all three metals are shown in Table 1.

In spite of careful monitoring of the reduction process, both compounds **1** and **2**, show only one species which gives rise to highly resolved NMR spectra. The total change in chemical shift of the diamagnetic species of **1**, *ca.* 560 ppm (553, 567 and 557 ppm for lithium, sodium and potassium, respectively), points to the formation of a tetraanionic species with a typical K_c value of *ca.* 140. The protons in the *ortho* and *meta* position on the phenyl moieties show four different chemical shifts. It is clear from the number of signals that in the tetraanion the rotation of the phenyls about the C-3′–C-2′ bond is slow (in the NMR timescale). The coupling constant of the ethylene protons, $^3J_{HH}$ 12.3 Hz, is intermediary between typical *cis* and *trans* values. There is a change in bond order due to delocalization of charge. It can be deduced from the correlation of ^{13}C NMR chemical shifts and local charge densities that the excess charge is delocalized over the entire molecule with the highest charge densities on carbon C-2′ and at the *para* and *ortho* positions of the phenyl moieties (Fig. 1). Charge densities in these positions, *i.e.* on the former double bond and *ortho* and *para* positions, in analogous systems are common.[7] The exception in this case is the relatively low charge density on the central ring. Such a behaviour may result from the strong interaction inside the cyclophane hub.

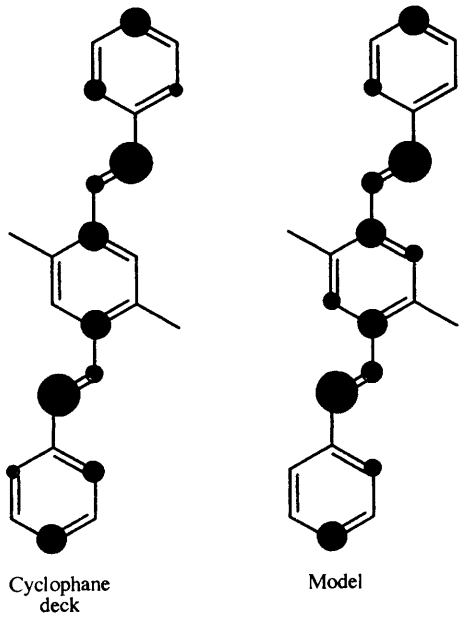

Fig. 1 Charge distribution according to NMR chemical shifts

Although there are slight differences in the chemical shifts, the charge distribution with all three alkali metals is practically similar (Table 1). The total chemical shift order in ^{13}C NMR, *i.e.* Na > K > Li, points to a different behaviour of the system when reduced with lithium. It might be due to the differences in ion-pairing equilibria of **1**, which forms contact ion pairs (cip) with sodium and potassium, and solvent separated ion pair (ssip) with lithium. These results were supported by the UV–VIS studies (*vide infra*).

The changes in the chemical shifts of **1** were compared with a charged model compound, *i.e.* **4**. Such a model compound is composed of the components of a single modified deck of the cyclophane. In view of the close structural relationship, the

Table 2 Displacement of carbon and proton chemical shifts (ppm) upon reduction of **4** with lithium

	4	3	5	2	6	1	7	8	9/12	10/13	11/14	CH_3	$\Sigma\delta\Delta$
Proton	1.93	0.98	1.16	1.39	1.59	—	2.53	1.90	—	1.72	—	0.70	30.6
Carbon	22.3	0.3	1.6	14.8	6.4	−5.0	45.6	17.6	21.7	11.6	7.3	−2.0	284.5

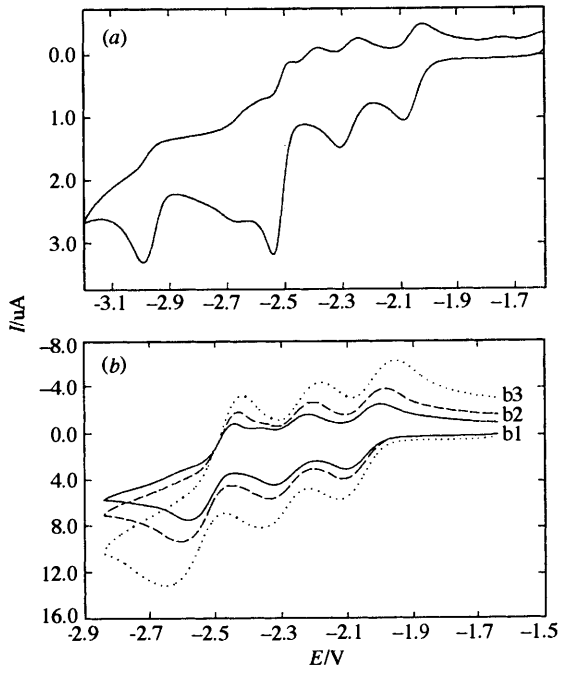

Fig. 2 Cyclic voltammogram for the reduction of **1** [$v = 0.1$ Vs^{-1} (*a*), 1 Vs^{-1} (b1), 2 Vs^{-1} (b2), and 5 Vs^{-1} (b3), at $t = -15$ °C]

NMR chemical shifts of most protons of the model are rather similar to those of **1**. As expected from the shielding effects generally observed for [2.2]paracyclophanes,[8] the protons H-5/8 in **1** resonate at a relatively higher field than the respective nuclei in the model compound. The signals of the protons of the terminal phenyl rings in **1** do not experience anisotropic shielding effects and therefore closely represent those in the model. It follows that the expected charge distribution should be the same, provided that the through space interaction of the cyclophane hub is excluded. The changes in chemical shifts of the model system upon charging with lithium are shown in Table 2. As has been shown previously, this stilbenoid system can be reduced to a stable dianion.[9] We encounter in **4** a total change in the carbon chemical shift of 284 ppm, half the value observed in compound **1** and **2**, which confirms that the cyclophanes are quadruply charged. Similar to compounds **1** and **2**, the coupling constant of the 'former' ethylene protons of **4** changes from $^3J_{HH}$ 16.2 Hz in the neutral system to $^3J_{HH}$ 12.4 Hz in the dianion salt. Different chemical shifts for the two *ortho* and two *meta* protons on the phenyl ring point to an increase in the barrier for the rotation of the phenyls about the C-2′–C-3′ bond, as a result of delocalization of charge which changes the bond order. Unlike the cyclophane, the charge densities on the central ring of **4** are slightly higher on the one hand, and are relatively lower on the double bond and the phenyl substituents on the other hand. Assuming an unperturbed behaviour for the charged model, the observed difference in the charge distribution can be ascribed to the through space effect of the cyclophane hub.

Electrochemical studies

The reactivity of the anionic species derived from **1** can also be demonstrated by cyclic voltammetry. However, a direct comparison with the chemical reduction is impossible in view of the lack of a counter cation in cyclic voltammetry. The cyclic voltammogram of **1** (Fig. 2) in tetrahydrofuran (THF) with Bu_4NPF_6 as supporting electrolyte shows four redox steps ($E^1_{1/2} = -2.05$, $E^2_{1/2} = -2.27$, $E^3_{1/2} = -2.52$, $E^4_{1/2} = -2.99$ V). The first reduction step, which is clearly reversible, occurs at a potential which is substantially less negative than that of the [2.2]paracyclophane ($E^1_{1/2} = -3.00$ V *vs.* standard calomel electrode, SCE).[10] It seems that the uptake of an electron becomes easier upon the extension of the π system. The reduction of compound **1** occurs more readily than the reduction of the model system ($E^1_{1/2} = -2.25$, $E^2_{1/2} = -2.54$ V). Due to the stabilizing influence of the two benzene rings, the lowest antibonding orbital which takes up the extra electron on passing from the neutral compound to its radical anion is more stable in compound **1** than in the model compound. The third and the fourth redox steps, which are not reversible under these conditions [Fig. 2(*a*)], point to an increase of the cathodic peak and a slight decrease of the anodic peak. This effect, which is pronounced in the third reduction step, is familiar in multi-step reduction processes.[11] A trace of water in the electrochemical cell may cause protonation of the redox product $\mathbf{1}^{3-}$, which can be further reduced immediately at almost the same potential. The stability of these protonated products is responsible for the decrease in the anodic peak upon oxidation. Protonations do not occur in the first two reduction steps, because of the low nucleophilicity of the species as a result of the low reduction potential of the redox products. As can be expected from such a redox mechanism, when the scanning becomes fast relative to the rate of the protonation process, the effect of a pronounced cathodic peak will decrease, as can be seen in Fig. 2(*b*). Although the cyclic voltammogram indicates four redox steps which lead to the tetraanion, it is still not clear why the intermediate dianion could not be detected by NMR spectroscopy, while the tetraanion gives rise to highly resolved NMR spectra. It should be noted that cyclophanes with less than three bridging carbon atoms allow the unpaired electron to undergo an exchange between the two decks.[12] In view of these observations a through space exchange of electrons should be taken into account.

UV–VIS spectroscopy

As can be expected from the molecular orbital analysis of the parent molecule [2.2]paracyclophane,[13] the electronic spectra of charged **1** in THF are basically different from those of charged **4** (our model compound). The spectra of **1** indicate only two different species upon charging (Fig. 3). The first stage is the formation of a radical anion, *i.e.* $\mathbf{1}^-$ [Fig. 3(*b*)], which is paramagnetic and cannot be observed by NMR. The UV–VIS spectrum of this radical anion is quite similar to the spectrum of the radical of the model system, **4**.[19] Contrary to **4**, we could not get a highly resolved EPR spectrum of this radical stage in **1**. The last reduction stage appears simultaneously with the appearance of the NMR spectrum and does not change after prolonged contact with the alkali metals [Fig. 3(*d*)]. In analogy to the dianionic state of the model, this diamagnetic species is ascribed to the tetraanion. In all other stages of reduction after the appearance of the radical species, both spectra of the radical ion and the tetraanion can be seen together. As the reduction progresses, there is an increase of the long-wave absorption, without any change in the absorption of the radical [Fig. 3(*c*)]. Continuation of the reduction after this stage showed a decrease of the signal of the radical species, and finally only the tetraanion is observed. By assuming that in the tetraanion salt, each deck is doubly charged, one should consider in all other stages a situation of fast electron exchange

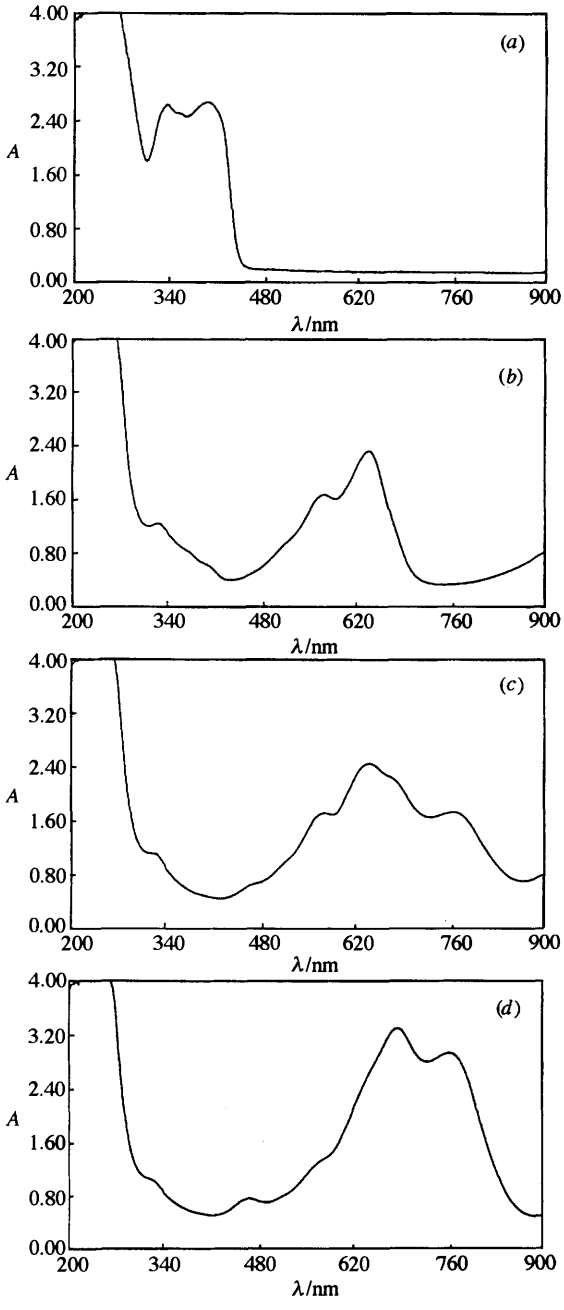

Fig. 3 The UV–VIS spectra of the reduction stages of cyclophane **1**

between two states, radical and dianion decks. Such an exchange can explain why it is not possible to see the signals of the dianion in the NMR spectrum, and why it is possible to see both the radical and the dianion species in the UV–VIS spectrum. In view of the above and the electrochemistry of the reduction of **1**, we suggest a stepwise process as shown in Scheme 1.

Ion solvation equilibria

The concept of an equilibrium between contact ion-pairs (cip), and solvent separated ion-pairs (ssip) is well established.[14] Usually, an increased size of the counterion in contact ion-pairs leads to a red shift of the UV–VIS bands. In the case of **1**, a blue shift[19] was found when Li^+ was replaced by K^+. This observation, although seemingly inconsistent with general theory, is not unusual. This is normally the case when ion-solvation equilibrium is shifted from cip in the potassium salt, to ssip in the lithium salt.[15] The red shift associated with the conversion of a contact ion-pair into a solvent separated ion-pair is analogous to that arising from increasing the size of a cation in a contact ion-pair.

The UV–VIS spectra of the alkali metal salts in THF, in each stage of charging, show two absorption peaks.[19] As the temperature was decreased, the spectrum drastically changed as shown in Fig. 4. These reversible changes of the absorption spectrum prove that the two species (cip and ssip) coexist in equilibrium. The absorption spectrum of an ionic species as contact ion pairs (cip) differs from that of the respective solvent separated ion pairs (ssip). Therefore, the change in the absorption spectrum is related to the modification of the relative concentration of cip and ssip. The same effect, although weaker, was observed while changing the cation from potassium (high tendency to form cip), to lithium (high tendency to form ssip), and by changing the solvent from diethyl ether to DME. An increase of the polarity of the solvent leads to better solvation of the cation and hence to greater dispersion of the cation charge and shifts the equilibrium to ssip. The observed solvent effect is significant when the cation is potassium.

^{7}Li NMR spectroscopy

The chemical shifts of the lithium cation are directly related to the ion solvation equilibria and to the nature of the charged species.[16] While the sensitivity of the ^{7}Li chemical shifts to the anion depends on the proximity of the anion and the cation in solution, the direction of the chemical shift is mainly influenced by shielding effects. Therefore, the lithium cation chemical shift affords information on ion-pairing equilibria and the magnetic properties of the anionic system. The lithium spectra were measured using an external standard of 0.1 M LiBr/THF. The ^{7}Li NMR spectrum of the tetraanion salt at different temperatures consists of only one broad line at −1.2 ppm (Fig. 5). One signal does not necessarily point to a full symmetry between the lithium cations; it can be due to a fast exchange in the NMR timescale, which is the usual case. Chemical shifts of −1.2 ppm originate from a solvent separated lithium cation, and only a weak contribution of the induced magnetic field is observed. In view of the above, it seems that the lithium cations do not dwell close to the cyclophane hub. Location of the lithium cations inside or above the cyclophane centre would cause a high-field shift of the ^{7}Li absorption line as a result of the strong shielding of the lithium by the ring current within the cyclophane hub.

Semiempirical MNDO molecular orbital calculations including the lithium atoms have been carried out for the tetraanion of **1**.[17] Although the calculations do not take solvation into account, they can provide further support for the approximate location of the lithium cations. Searching for the minimum energy for different positions of the lithium cation around the anion system, we found a few structures with almost the same energy. In all these structures, the lithium cations dwell near the external carbon–carbon bonds (Fig. 6). The structures in which the lithium cations were close to the cyclophane centre, were of higher energy.

Conclusions

The reduction of **1** and **2** yielded tetraanions—two electrons on each 'deck'. The systems, being crossed layered hydrocarbons, show interesting charge delocalization properties. The through-space effect operating between the layers shifts the charge to the molecular periphery. It seems that the structure of the crossed cyclophane facilitates the charge delocalization towards the periphery.

Experimental

All NMR analyses were performed on a Bruker AMX-400 pulsed FT spectrometer, operating at 400.13 and 100.62 MHz for ^{1}H and ^{13}C NMR, respectively. *J* values are given in Hz. UV–VIS spectra were recorded on a UVIKON 860 KONTRON spectrometer.

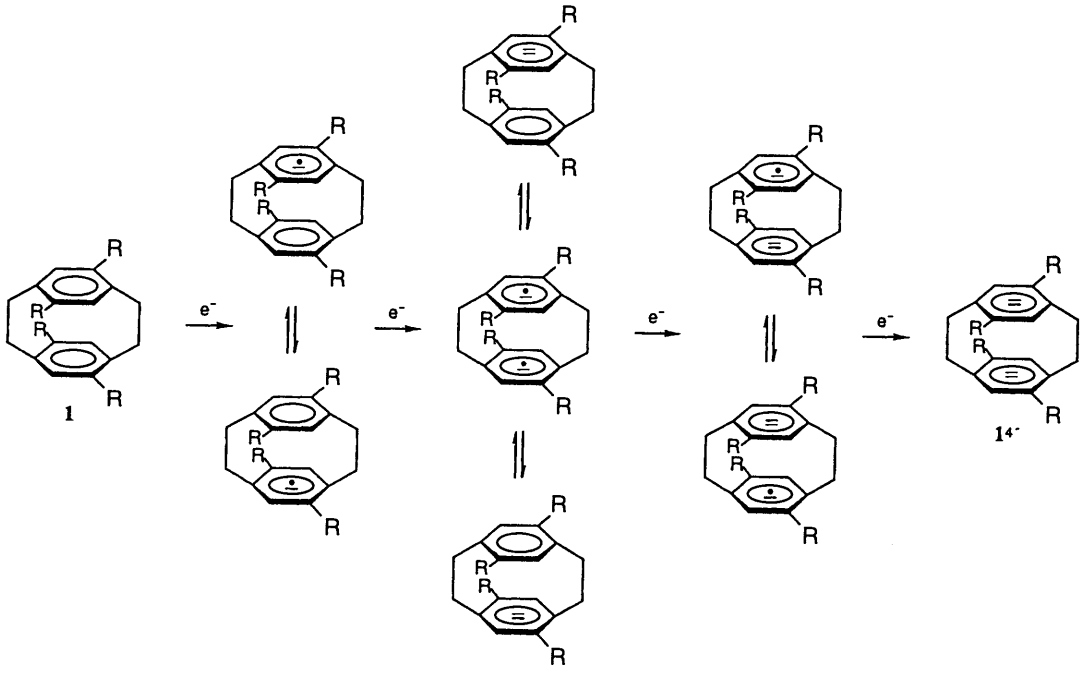

Scheme 1 Stepwise charging of **1**

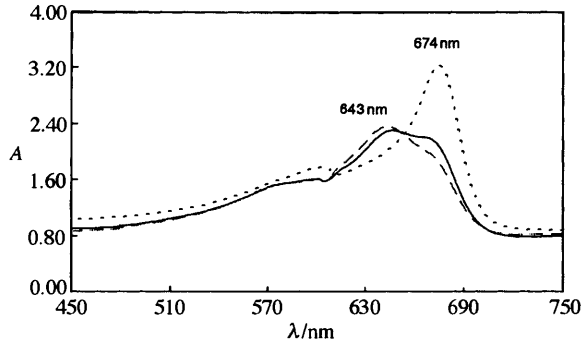

Fig. 4 Change of UV–VIS spectrum of the radical anion as a function of temperature; —— 17 °C, – – – 34 °C, ------ −60 °C

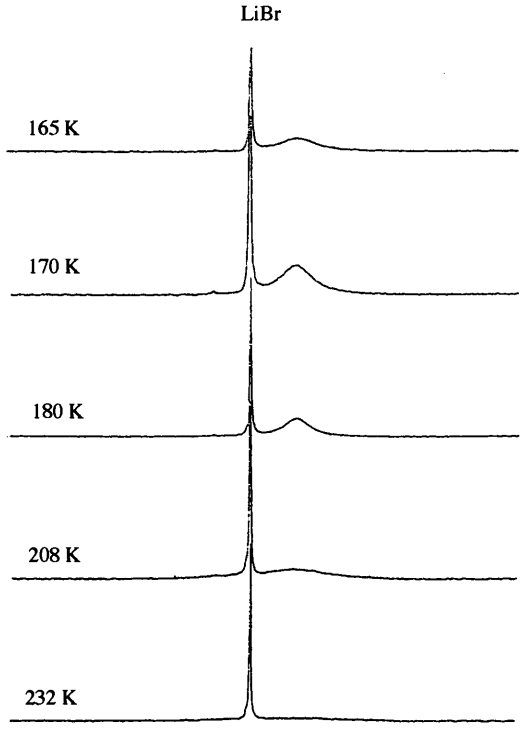

Fig. 5 The influence of the temperature on the ^{7}Li NMR spectrum of the cyclophane tetraanion

Electrochemical studies

All electrochemical measurements were carried out at *ca.* −15 °C, in a three compartment electrode cell with a gold wire (d = 1 mm, sealed in glass) as a working electrode, and a platinum wire concentrically wound around the working electrode as a counter electrode. A silver wire was used as a quasi-reference electrode calibrated with Fc/Fc^+ to be 0.310 V *vs.* SCE or $Co(C_5H_5)^+PF_6$ to be 1.040 V *vs.* SCE. The background solution (0.1 M Bu_4NPF_6 in THF) was used for the measurement of 10^{-5}–10^{-4} M substrate. The oxygen was removed by bubbling argon. All potentials were reported with respect to standard calomel electrode (SCE).

Materials

Potassium, sodium and lithium (Aldrich) were kept in paraffin oil and were rinsed shortly before using with light petroleum (bp 40–60 °C). [$^2H_8$]THF (Aldrich) was dried over potassium–sodium alloy under vacuum. All cyclophane compounds (**1**, **2**, **3**) as well as the model system **4** were prepared according to published procedures.[3,18]

General procedure for the reduction process

Lithium wire, sodium or potassium mirror were introduced to the upper part of an extended NMR tube containing the cyclophane (10^{-2} M) dissolved in [$^2H_8$]THF. The sample was degassed and sealed under vacuum. The solution was brought into contact with the metal solution by turning the tube upside down.

Quenching of the anions

All anions were quenched with oxygen. The quenching experiments were carried out by bubbling oxygen gas into the NMR sample tube under anhydrous conditions. Oxygen gas was slowly bubbled *via* a syringe into the cold anion solution, the deep colour disappeared and the ^{1}H NMR spectrum was recorded.

NMR Spectra

4,7,12,15-Tetrastyryl[2.2]paracyclophane (1). δ_H(400 MHz,

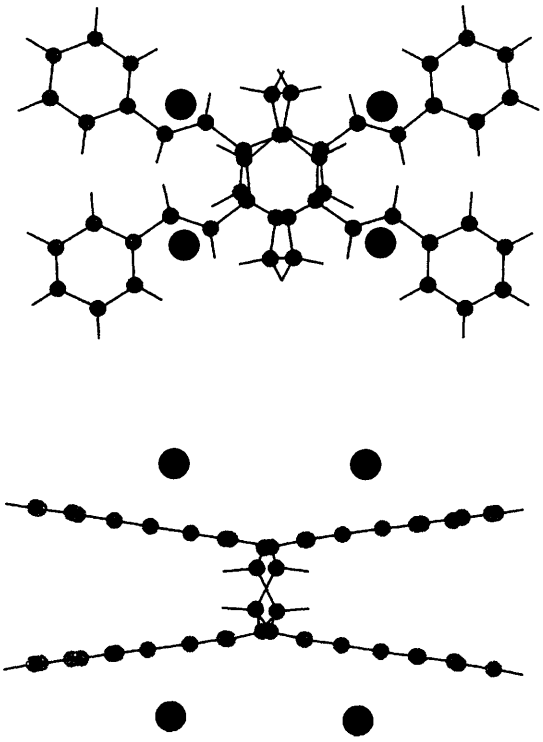

Fig. 6 Location of the lithium cations as obtained from MNDO calculations

[$^2H_8$]THF, 295 K) 7.34 (4 H, t, J_{HH} 7.3, 6′-H), 7.45 [8 H, dd, J_{HH} 7.3, 5′(7′)-H], 7.61 [8 H, d, J_{HH} 7.3, 4′(8′)-H], 7.05 (4 H, d, J_{HH} 16.3, 2′-H), 7.43 (4 H, d, J_{HH} 16.3, 1′-H), 7.13 [4 H, s, 5(8)-H], 3.74 3.01 (8 H, m, CH_2), δ_C 127.96 (C-6′), 129.17 [C-5′(7′)], 127.27 [C-4′(8′)], 138.64 (C-3′), 129.20 (C-2′), 126.13 (C-1′), 137.53 [C-4(7)], 128.74 [C-5(8)], 138.64 [C-3(6)], 33.42 [C-2(9)].

Lithium salt (1^{4-}/4Li^+). δ_H(400 MHz, [$^2H_8$]THF, 220 K) 5.14 (4 H, dd, J_{HH} 7.0, 7.6, 6′-H), 6.30 (4 H, dd, J_{HH} 7.6, 8.3, 5′-H), 6.10 (4 H, dd, J_{HH} 7.0, 8.2, 7′-H), 6.20 (4 H, d, J_{HH} 8.3, 4′-H), 5.88 (4 H, d, J_{HH} 8.2, 8′-H), 4.24 (4 H, d, J_{HH} 12.3, 2′-H), 5.79 (4 H, d, J_{HH} 12.3, 1′-H), 5.40 [4 H, s, 5(8)-H], 2.70 2.56 [8 H, m, 2(9)-H]. δ_C 103.39 (C-6′), 128.77 (C-5′), 127.37 (C-7′), 111.83 (C-4′), 119.93 (C-8′), 144.49 (C-3′), 81.30 (C-2′), 112.68 (C-1′), 117.02 [C-4(7)], 123.65 [C-5(8)], 130.39 [C-3(6)], 34.04 [C-2(9)]. ^{7}Li NMR (170 K) δ_{Li} −1.1 ppm.

Sodium salt (1^{4-}/4Na^+). δ_H(400 MHz, [$^2H_8$]THF, 220 K) 5.38 (4 H, dd, J_{HH} 7.0, 7.3, 6′-H), 6.40 (4 H, dd, J_{HH} 7.3, 8.2, 5′-H), 6.23 (4 H, dd, J_{HH} 7.0, 7.8, 7′-H), 6.33 (4 H, d, J_{HH} 8.2, 4′-H), 6.08 (4 H, d, J_{HH} 7.8, 8′-H), 4.40 (4 H, d, J_{HH} 12.6, 2′-H), 5.89 (4 H, d, J_{HH} 12.6, 1′-H), 5.30 [4 H, s, 5(8)-H], 2.79 2.59 [8 H, m, 2(9)-H]. δ_C 106.10 (C-6′), 128.78 (C-5′), 127.53 (C-7′), 112.35 (C-4′), 120.60 (C-8′), 144.72 (C-3′), 79.81 (C-2′), 111.85 (C-1′), 113.76 [C-4(7)], 120.60 [C-5(8)], 131.66 [C-3(6)], 33.71 [C-2(9)].

Potassium salt (1^{4-}/4K^+). δ_H(400 MHz, [$^2H_8$]THF, 220 K) 5.37 (4 H, dd, J_{HH} 7.3, 7.8, 6′-H), 6.42 (4 H, dd, J_{HH} 7.3, 8.3, 5′-H), 6.42 (4 H, dd, J_{HH} 7.3, 8.3, 5′-H), 6.25 (4 H, dd, J_{HH} 7.2, 8.2, 7′-H), 6.34 (4 H, d, J_{HH} 8.3, 4′-H), 5.95 (4 H, d, J_{HH} 8.2, 8′-H), 4.20 (4 H, d, J_{HH} 12.2, 2′-H), 5.91 (4 H, d, J_{HH} 12.2, 1′-H), 5.28 [4 H, s, 5(8)-H], 2.77 2.54 [8 H, m, 2(9)-H]. δ_C 105.89 (C-6′), 129.19 (C-5′), 128.52 (C-7′), 112.15 (C-4′), 118.28 (C-8′), 143.47 (C-3′), 81.77 (C-2′), 112.50 (C-1′), 115.01 [C-4(7)], 122.69 [C-5(8)], 131.15 [C-3(6)], 33.29 [C-2(9)].

Tetramethyl derivative (2). δ_H(400 MHz, [$^2H_8$]THF, 295 K) 2.09 [12 H, s, (8′)Me], 7.09 (4 H, d, J_{HH} 7.6, 7′-H), 7.12 (4 H, dd, J_{HH} 7.3, 7.6 Hz, 6′-H), 7.21 (4 H, dd, J_{HH} 7.3, 7.6, 5′-H), 7.77 (4 H, d, J_{HH} 7.6, 4′-H), 7.14 (4 H, d, J_{HH} 16.0, 2′-H), 7.23 (4 H, d, J_{HH} 16.0, 1′-H), 7.05 [4 H, s, 5(8)-H], 3.67 2.99 [8 H, m, 2(9)-H]. δ_C 19.65 [C-(8′)Me], 136.50 (C-8′), 130.82 (C-7′), 127.84 (C-6′), 126.66 (C-5′), 125.83 (C-4′), 137.49 (C-3′), 126.86 (C-2′), 127.59 (C-1′), 137.97 [C-4(7)], 129.32 [C-5(8)], 138.59 [C-3(6)], 33.45 [C-2(9)].

Sodium salt (2^{4-}/4Na^+). δ_H(400 MHz, [$^2H_8$]THF, 295 K) 1.71 [12 H, s, (8′)Me], 6.27 (4 H, d, J_{HH} 6.3, 7′-H), 5.49 (4 H, dd, J_{HH} 6.3, 7.6, 6′-H), 6.42 (4 H, dd, J_{HH} 7.6, 8.2, 5′-H), 6.61 (4 H, d, J_{HH} 8.2, 4′-H), 4.12 (4 H, d, J_{HH} 12.2, 2′-H), 6.14 (4 H, d, J_{HH} 12.2, 1′-H), 5.37 [4 H, s, 5(8)-H], 2.89 2.69 [8 H, m, 2(9)-H]. δ_C 21.30 [C-(8′)Me], 123.26 (C-8′), 128.56 (C-7′), 105.74 (C-6′), 125.94 (C-5′), 112.48 (C-4′), 142,56 (C-3′), 77.28 (C-2′), 112.61 (C-1′), 114.39 [C-4(7)], 120.72 [C-5(8)], 131.80 [C-3(6)], 33.73 [C-2(9)].

Potassium salt (2^{4-}/4K^+). δ_H(400 MHz, [$^2H_8$]THF, 295 K) 1.77 [12 H, s, (8′)Me], 6.31 (4 H, d, J_{HH} 6.4, 7′-H), 5.52 (4 H, dd, J_{HH} 6.4, 7.3, 6′-H), 6.45 (4 H, dd, J_{HH} 7.3, 8.3 Hz, 5′-H), 6.59 (4 H, d, J_{HH} 8.3, 4′-H), 3.98 (4 H, d, J_{HH} 12.0, 2′-H), 6.12 (4 H, d, J_{HH} 12.0, 1′-H), 5.30 [4 H, s, 5(8)-H], 2.93 2.66 [8 H, m, 2(9)-H]. δ_C 21.04 [(C-(8′)Me], 122.24 (C-8′), 129.07 (C-7′), 106.49 (C-6′), 126.30 (C-5′), 112.22 (C-4′), 141.71 (C-3′), 77.45 (C-2′), 112.40 (C-1′), 116.17 [C-4(7)], 122.17 [C-5(8)], 132.02 [C-3(6)], 33.17 [C-2(9)].

Tetramethoxy derivative (3). δ_H(400 MHz, [$^2H_8$]THF, 295 K) 6.93, 7.46 [16 H, d, J_{HH} 8.7, 5′(7′)-H, 4′(8′)-H], 6.88 (4 H, d, J_{HH} 16.3, 2′-H), 7.16 (4 H, d, J_{HH} 16.3, 1′-H), 6.98 [4 H, s, 5(8)-H], 3.82 (12 H, s, OMe), 3.58, 2.86 (8 H, m, CH_2).

2,5-Dimethyl-1,4-distyrylbenzene (4). δ_H(400 MHz, [$^2H_8$]-THF, 295 K) 7.55 [4 H, d, J_{HH} 7.6, 2(6)-H], 7.32 [4 H, dd, J_{HH} 7.4, 7.6 Hz, 3(5)-H], 7.21 (2 H, t, J_{HH} 7.4, 4-H), 7.09 (2 H, d, J_{HH} 16.2, 7-H), 7.39 (2 H, d, J_{HH} 16.2, 8-H), 7.49 [2 H, s, 10(13)-H], 2.43 [6 H, s, 11(14)Me]. δ_C 138.71 (C-1), 127.07 [C-2(6)], 129.12 [C-3(5)], 127.93 (C-4), 129.95 (C-2), 126.49 (C-8), 136.18 [C-9(12)], 127.60 [C-10(13)], 134.03 [C-11(14)], 19.31 [C-11-(14)Me].

Lithium salt (4^{2-}/2Li^+). δ_H(400 MHz, [$^2H_8$]THF, 220 K) 5.96 (2 H, d, J_{HH} 7.3, 2-H), 6.16 (2 H, dd, J_{HH} 7.0, 7.3, 3-H), 5.28 (2 H, dd, J_{HH} 6.8, 7.0, 4-H), 6.34 (2 H, dd, J_{HH} 6.8, 7.0, 5-H), 6.16 (2 H, d, J_{HH} 7.0, 6-H), 4.56 (2 H, d, J_{HH} 12.4, 7-H), 5.49 (2 H, d, J_{HH} 12.4, 8-H), 5.77 [2 H, s, 10(13)-H], 1.73 [6 H, s, 11(14)Me]. δ_C 143.8 (C-1), 120.66 (C-2), 127.49 (C-3), 105.25 (C-4), 128.81 (C-5), 112.23 (C-6), 84.33 (C-7), 108.90 (C-8), 114.45 [C-9(12)], 116.02 [C-10(13)], 126.75 [C-11(14)], 21.28 [C-11(14)Me]. δ_{Li} 1.2 ppm.

Acknowledgements

We are thankful to Professor K. Müllen and Dr Eugenii Katz for electrochemical measurements and fruitful discussions. Financial support granted by the Research and Development Authority of the Hebrew University of Jerusalem is gratefully acknowledged.

References

1 H. Hope, J. Bernstein and K. N. Trueblood, *Acta. Crystallogr., Sect. B*, 1972, **28**, 1733.
2 J. M. Robertson, in *Organic Crystals and Molecules*, Cornell University Press, Ithaca, 1953.
3 B. König, B. Knieriem and A. de Meijere, *Chem. Ber.*, 1993, **126**, 1643.
4 S. Misumi in *Cyclophanes*, ed. Keehn, Academic Press, New York, 1983, vol II, p. 579.
5 (*a*) G. Fraenkel, R. E. Carter, A. McLachlan and J. H. Richards, *J. Am. Chem. Soc.*, 1960, **82**, 5846; (*b*) D. G. Farnum, in *Adv. Phys. Org. Chem.*, eds. V. Gold and D. Bether, Academic Press, London, 1975, vol. 1, p. 123; (*c*) B. Eliasson, U. Edlund and K. Müllen, *J. Chem. Soc., Perkin Trans. 2*, 1986, 937; (*d*) K. Müllen, *Chem. Rev.*, 1984, **84**, 603.
6 D. Tamarkin and M. Rabinovitz, unpublished results.
7 (*a*) A. Böhm and K. Müllen, *Tetrahedron Lett.*, 1992, **33**, 611; (*b*) A. Weitz, unpublished results.
8 D. J. Cram, C. K. Dalton and G. R. Knox, *J. Chem. Soc.*, 1963, **85**, 1088.

9 R. Schenk, H. Gregorius, K. Meerholz, J. Heinze and K. Müllen, *J. Am. Chem. Soc.*, 1991, **113**, 2634.
10 R. June, P. Lemoine and M. Gross, *Angew. Chem.*, 1982, **94**, 312; *Agnew. Chem., Int. Ed. Engl.*, 1982, **21**, 305.
11 B. A. Kiseler, Y. N. Kozlov and V. B. Erstigneer, *Biofizika*, 1974, **19**, 645 (in Russian).
12 F. Gerson, *Top. Curr. Chem.*, 1983, **115**, 57.
13 (*a*) E. Heilbronner, *Top. Curr. Chem.*, 1983, **115**, 1; (*b*) F. Gerson, *Top. Curr. Chem.*, 1983, **115**, 57.
14 T. E. Hogen-Esch and J. Smid, *J. Am. Chem. Soc.*, 1966, **88**, 307.
15 M. Szwarc, *Carbanion Living Polymer and Electron Transfer Processes*, Wiley, New York, 1968.
16 (*a*) R. H. Cox, H. W. Terry, Jr. and L. W. Harrison, *Tetrahedron Lett.*, 1971, **50**, 4815; (*b*) R. H. Cox and H. W. Terry, Jr., *J. Magn. Reson.*, 1974, **14**, 317; (*c*) R. H. Cox, H. W. Terry, Jr. and L. W. Harrison, *J. Am. Chem. Soc.*, 1971, **93**, 3297.
17 MNDO-MOPAC Version 6 J. J. P. Stewart, *QCPE Bull.*, **3**, 1983, 455.
18 T. W. Campbell and R. N. McDonald, *J. Am. Chem. Soc.*, 1959, **4**, 1246.
19 UV–VIS absorptions. Neutral compound **1**: $\lambda = 284$, 340 and 392 unm. $\mathbf{1}^{-}/Li^{+}$: λ 673 and 588 nm, $\mathbf{1}^{-}/K^{+}$: λ 648 and 568 nm, $\mathbf{1}^{4-}/4Li^{+}$: λ 795 and 699 nm, $\mathbf{1}^{4-}/4K^{+}$:λ 751 and 682 nm.

Paper 6/04277E
Received 18*th June* 1996
Accepted 30*th July* 1996